arXiv:astro-ph/0504148v1 6 Apr 2005

X-ray Variability of Active Galactic Nuclei and the Flare Model

R.W. Goosmann [a], B. Czerny [b], A.-M. Dumont [a], M. Mouchet [a], A. Różańska [b], V. Karas [c,d], and M. Dovčiak [d]

[a] *LUTH, Observatoire de Paris, Meudon, 5 place Jules Janssen, 92190 Meudon, France*

[b] *Nicolaus Copernicus Astronomical Center, Bartycka 18, 00-716 Warsaw, Poland*

[c] *Charles University, Faculty of Mathematics and Physics, Ke Karlovu 3, 121 16 Prague 2, Czech Republic*

[d] *Astronomical Institute, Academy of Sciences, Narodni 3, 117 20 Prague 1, Czech Republic*

Abstract

Short-term variability of X-ray spectra has been reported for several Active Galactic Nuclei. Significant X-ray flux variations are observed within time scales down to 10^4—10^5 seconds. We discuss short variability time scales in the framework of the X-ray flare model, which assumes the release of a large hard X-ray flux above a small portion of the accretion disk. The resulting observed X-ray spectrum is composed of the primary radiation as well as a reprocessed/Compton reflection component that we model performing numerical radiative transfer simulations. We conduct Monte-Carlo simulations of large flare distributions across the disk including relativistic corrections of the observed radiation and discuss general implications on AGN spectra and their variability.

Key words: galaxies: active, X-rays: galaxies, accretion disks, radiative transfer

1 Introduction

The X-ray emission of Active Galactic Nuclei (AGN) can be explained by two components: a primary radiation emerging from a hot, optically thin medium

Email address: rene.goosmann@obspm.fr (R.W. Goosmann).

and a reprocessed component coming from colder, optically thick medium. The existence of these two media can be explained by the flare model, which was first suggested by Galeev, Rosner, & Vaiana (1979) and developed in many subsequent papers for both galactic black holes and AGN. The AGN flares are assumed to be driven similarly to solar flares: magnetic reconnection creates a compact source above the accretion disk, the source emits the primary spectrum partly reaching the observer directly and partly illuminating the disk atmosphere, the atmosphere then emits the reprocessed spectrum.

In this paper we present the first modeling results for the reprocessed radiation coming from the irradiated area, the so-called hot-spot, underneath a compact flare source as indicated in Fig. 1. We take into account details of the flare geometry including the dependence on the incident angle of the primary radiation.

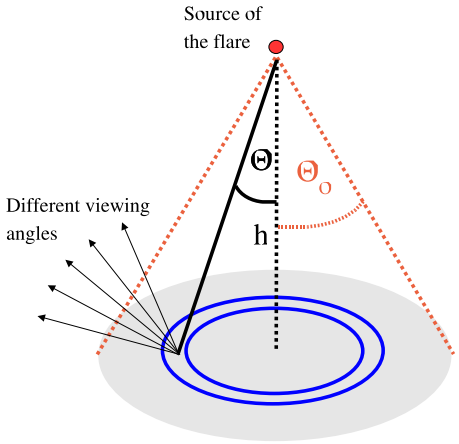

Fig. 1. Flare geometry

We further conduct Monte-Carlo simulations of random flare distributions across the accretion disk in order to construct rms X-ray spectra. These simulations also contain relativistic corrections due to the curved space-time in the vicinity of the black hole. We show general trends for several parameters such as the radial distribution of hot-spots and of the incident radiation flux over the disk.

2 Modeling

2.1 The reprocessed spectra across the hot-spot

We perform detailed radiative transfer using the codes *TITAN* and *NOAR* described in Dumont, Abrassart, & Collin (2000) and in Dumont et al. (2003).

TITAN conducts radiative transfer inside optically thick media, determining the temperature and ionization structure. *NOAR* is a Monte-Carlo code treating the Compton processes. We consider a plane-parallel section of the accretion disk atmosphere at 18 R_g ($R_g = \frac{GM}{c^2}$, M being the mass of the black hole) from the disk center. The hydrostatic equilibrium of such an atmosphere is calculated following Różańska et al. (1999) assuming a 10^8 solar mass black hole and an Eddington accretion rate of 0.001. Collin et al. (2003) have shown that a change of the hydrostatic equilibrium due to the onset of the flare happens slowly compared to the adjustment of the temperature and ionization profile inside the medium. We therefore assume that the density structure of the medium does not change for a significant fraction of the total flare duration.

For the incident flux F_{inc} we presume a power law with $F_{inc} \propto E^{-\alpha}$, $\alpha = 0.9$, between 0.1 eV and 100 keV. The ratio F_{inc}/F_{disk} of the incident flux to the flux coming from the disk is fixed at 144, hence the flare by far dominates over the disk emission.

It can be seen from Fig. 1 that the incident angle and the ionization parameter $\xi = \frac{4\pi F_{inc}}{n_H}$ of the primary radiation (with F_{inc} being the incident flux and n_H being the hydrogen density at the disk surface) depend on the position within the hot-spot. This aspect has not yet been considered in previous flare models where the disk illumination was defined as semi-isotropic (Czerny et al., 2004; Collin et al., 2003) or with a constant incident angle (Nayakshin & Kallman, 2001).

For reasons of energy equipartition the distance h of the flare source above the disk surface should be similar to the pressure scale height of the disk (Galeev, Rosner, & Vaiana, 1979). Applying equation (2.8) of Shakura & Sunyaev (1973) to our case we derive $h \sim 1.9 \times 10^{11}$ cm $\sim 0.013\, R_g$. We define a half-opening angle $\Theta_0 = 60°$ for the flare cone, which, for an isotropically emitting source, corresponds to 50% of the incident flux reaching the disk being reprocessed. Then, the hot-spot radius of $h \times \tan 60° \sim 0.023\, R_g$ verifies our implicit assumption that the hydrostatic equilibrium computed at 18 R_g is sufficiently accurate across the whole hot-spot.

The observed spectrum is constructed as the integrated spectra of successive concentric rings at incident angles with $0° < \Theta < \Theta_0$. The spectra can be evaluated at various disk viewing angles i (measured from the disk symmetry axis). Details of the calculation method will be published in a following article (Goosmann et al., in preparation).

2.2 The rms-variability of random flare distributions

To investigate the consequences of this more detailed modeling of the hot-spot we perform Monte-Carlo simulations of many flares distributed over the accretion disk. The procedure is outlined in Czerny et al. (2004). We assume the hot-spot emission to be independent of the flare position. Radial probability distributions $p(R_i, \phi_i)$ for the appearance of a flare can be defined as

$$p(R_i, \phi_i) \equiv p(R_i)p(\phi_i) = \frac{(\gamma_{rad}+2)R_i^{\gamma_{rad}+1}}{R_{out}^{\gamma_{rad}+2} - R_{in}^{\gamma_{rad}+2}} \times \frac{1}{2\pi}. \quad (1)$$

Herein R_i and ϕ_i are polar coordinates, R_{in} and R_{out} denote the inner and the outer disk radius. For $\gamma_{rad} = 0$ the hot-spot distribution is uniform while for positive (negative) values of γ the number of flares rises in the outer (inner) disk part. We also enable a radial dependence of the hot-spot incident flux:

$$F_{inc} = F_0 \left[\frac{R_i}{R_{in}}\right]^{-\beta_{rad}}. \quad (2)$$

Since the dissipation within a Keplerian disk scales with r^{-3} we expect β_{rad} of the order of 3. Finally, the radial dependence of the flare life-time is chosen to scale with the Keplerian time scale.

The average number of hot-spots existing on the disk is denoted by n_{mean}, the mean X-ray luminosity of the primary source by $L_X = 8 \times 10^{43}$ erg s^{-1}. The rms-spectra are computed from $n_{seq} = 50$ consecutive model observations, each of an integration time $T_{integ} = 6156$ s. Relativistic effects are included by application of the code *KY* (see Dovčiak, Karas, & Yaqoob, 2004, for a code description). For the following computations we assume a Kerr black hole of 10^7 solar masses with spin parameter $a = 0.95$. The inner disk radius is at $1.8\,R_g$, the outer one at $50\,R_g$. The viewing angle of a distant observer is taken to be $i = 30°$.

3 Results

3.1 The reprocessed spectra across the hot-spot

In this paper we only examine the pure reprocessed component (e.g. without dilution by the primary radiation) for various positions within the hot-spot, e.g. for various incident angles of the irradiating flux. In Fig. 2 we show the

reprocessed flux EF_E versus photon energy E at several incident angles Θ. The results are shown for a face-on view, as assumed in Seyfert-1 galaxies, and for an intermediate viewing angle, as supposed for Seyfert-2 galaxies. For both viewing angles spectral variations are found in the soft X-rays across the hot-spot. These changes are more significant at higher viewing angles and affect the whole spectrum. Note that the dependence on the incident angle of the primary spectrum is opposite for the two viewing angles shown. At face-on view the flux decreases with rising incident angle, while at intermediate viewing angles it rises.

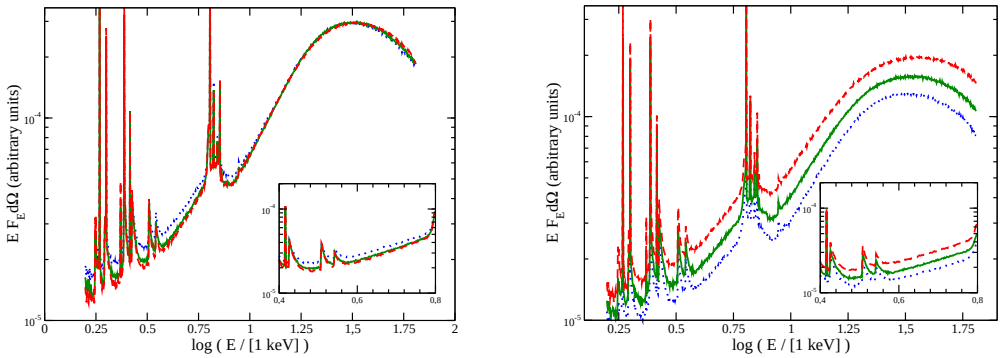

Fig. 2. Reprocessed spectra for different incident angles of the irradiating hard X-rays. Dotted line: $\cos\Theta = 0.95$ ($\Theta = 18°$). Solid line: $\cos\Theta = 0.65$ ($\Theta = 49°$). Dashed line: $\cos\Theta = 0.35$ ($\Theta = 70°$). Left: face-on view. Right: intermediate viewing angle at 62° from the normal. The inlets show a zoom between 0.4 and 0.8 keV.

The spectra emitted by the whole hot-spot are shown in Fig. 3. For increasing viewing angles the spectra decrease systematically, as does the soft X-ray slope and the ratio of the Compton hump to the soft X-ray spectrum.

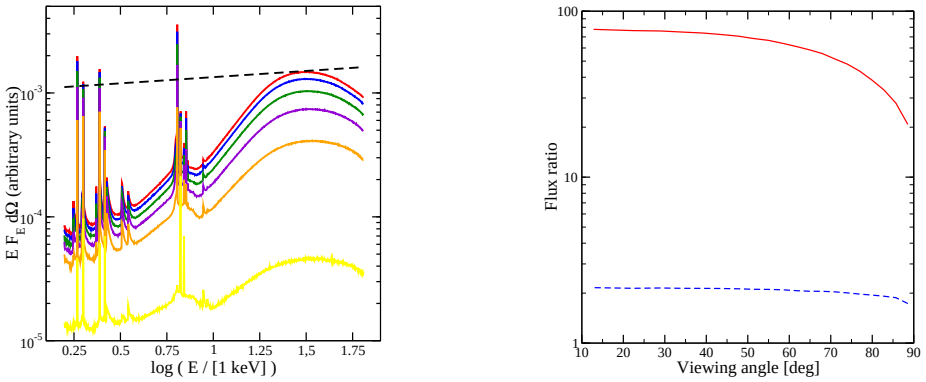

Fig. 3. Left: integrated spectra of a hot-spot with half-opening angle of 60°. The viewing angles increases from top ($i = 13°$) to bottom ($i = 89°$). Right: flux ratios versus viewing angle for such a hot-spot. Dashed line: F[5.5keV]/F[4keV] (soft X-ray slope). Solid line: F[28keV]/F[4keV] (hard/soft X-ray slope).

3.2 The rms-variability of random flare distributions

In Fig. 4 (left) we show the dependence of the rms spectra on the radial distribution of the incident radiation flux. Again, we do not consider any dilution by the primary radiation of the flare. We assume that the hot-spots at outer radii are dimmer, but if the decrease of the luminosity is fast, the rms spectrum has a much more complicated structure since it depends strongly on a few innermost brightest hot-spots. Computing various random realizations of the process without any variations in the model parameters, we see statistical differences between them. If the hot-spot's surface brightness decreases more slowly the role of the outer hot-spots increases, causing a major drop in the overall variability level.

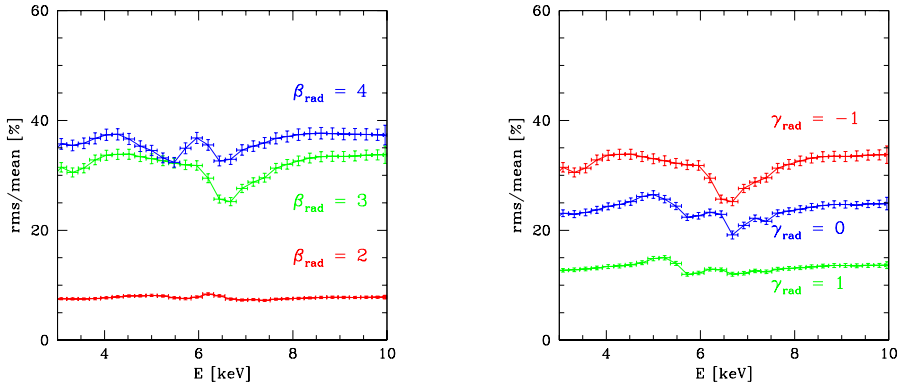

Fig. 4. Left: Dependence of the rms/mean spectrum on β_{rad} (other model parameters: $\gamma_{rad} = -1.5$, $n_{mean} = 300$). Right: Dependence of the rms/mean spectrum on γ_{rad} (other model parameters: $\beta_{rad} = 3$, $n_{mean} = 100$).

In Fig. 4 (right) the rms spectra for several radial hot-spot distributions are shown. The value of $\gamma_{rad} = 0$ corresponds to a random but uniform coverage of the disk surface by the hot-spots. If the flares and hot-spots appear more frequently in the outer part of the disk ($\gamma_{rad} > 0$), the overall variability decreases but a variable red wing is still present. If the flares appear relatively more frequently in the inner part of the disk ($\gamma_{rad}) < 0$, a clear dip is seen at the position of the unshifted iron line.

4 Discussion and Conclusions

Modeling the reprocessed radiation of the hot-spot reveals that the pure reflection component varies with the position in the hot-spot. This variation is

stronger for intermediate (edge-on) viewing angles than for a face-on viewing direction. The effect is caused by the ξ parameter varying with the distance from the hot-spot center. For outer parts of the hot-spot ξ is lower, it will thus cause a colder medium and a thinner hot surface of the atmosphere. The temperature of the medium determines its absorption properties, while the hot surface will influence, by electron scattering, the angular dependence of the re-emitted flux. The incident angle of the radiation also has an impact on the spectral shape as the Compton scattering phase function is not isotropic.

The integrated spectra show a strong dependence on the viewing direction. This effect is partly explained by the size of the projected surface area of the hot-spot seen at different inclinations. However, there also is a dependence of the overall spectral slope on the viewing direction that could be used to put observational constraints on the disk inclination.

The modeling of rms spectra for distributions of many flares across the disk reveals that flares at the inner part of the disk dominate the variability. Either a strong concentration of flares at the inner disk part or a relatively higher luminosity of inner disk flares increases the level of variability. Due to the light bending, an orbiting flare in the central region of the disk is effectively seen at various local viewing angles, which increases spectral variations. Although the overall level of variability is only weakly dependent on the energy, there are variations of the rms spectra for the energy range of the Kα line. This effect is due to the strong gravity close to the Kerr black hole. It could give a hint to the lack of variability in the iron Kα line observed in MCG -6-30-15 (see e.g. Fabian & Vaughan, 2003, and references therein).

A basic assumption of our modeling is that the density structure of the medium stays constant after the onset of the flare. Hence, we give results for flares having a short duration compared to the dynamical time scale. On longer time scales the medium expands to obtain a new hydrostatic equilibrium (see Czerny & Goosmann, 2004, for details) and the spectral properties change.

References

Collin, S., Coupé, S., Dumont, A.-M., Petrucci, P.-O., & Różańska, A. 2003, "Evolution of the X-ray spectrum in the flare model of Active Galactic Nuclei", A&A, 400, 437-449

Czerny, B., Różańska, A., Dovčiak, M., Karas, V., & Dumont, A.-M. 2004, "The structure and radiation spectra of illuminated accretion disks in AGN. II. Flare/spot model of X-ray variability", 'A&A, 420, 1-16

Czerny, B., & Goosmann, R. 2004, "Flare-induced fountains and buried flares in AGN", A&A, 428, 353-363

Dovčiak, M., Karas, V., & Yaqoob, T. 2004, "An Extended Scheme for Fitting

X-Ray Data with Accretion Disk Spectra in the Strong Gravity Regime", ApJS, 153, 205-221

Dumont, A.-M., Abrassart, A., & Collin, S. 2000, "A code for optically thick and hot photoionized media", A&A, 357, 823-838

Dumont, A.-M., Collin, S., Paletou, F., Coupé, S., Godet, O., & Pelat, D. 2003, "Escape probability methods versus "exact" transfer for modelling the X-ray spectrum of Active Galactic Nuclei and X-ray binaries", A&A, 407, 13-30

Fabian, A. C. & Vaughan, S. 2003, "The iron line in MCG-6-30-15 from XMM-Newton: evidence for gravitational light bending?", MNRAS, 340, L28-L32

Galeev, A. A., Rosner, R., & Vaiana, G. S. 1979, "Structured coronae of accretion disks", ApJ, 229, 318-326

Nayakshin, S. & Kallman, T. R. 2001, "Accretion Disk Models and Their X-Ray" Reflection Signatures. I. Local Spectra", ApJ, 546, 406-418

Różańska, A., Czerny, B., Życki, P. T., & Pojmański, G. 1999, "Thermal conduction between an accretion disc and a corona in active galactic nuclei: vertical structure of the transition layer", MNRAS, 305, 481-491

Shakura, N. I., & Sunyaev, R. A. 1973, "Black holes in binary systems. Observational appearance.", A&A, 24, 337-355